WCTE 2018
2018 World Conference on Timber Engineering
August 20 - 23, 2018 | Seoul, Republic of Korea

# FRAGILITY ANALYSIS OF A MASS-TIMBER FRAME STRUCTURE WITH RING-DOWELED MOMENT-RESISTING CONNECTIONS

**Leonardo Rodrigues[1], Luís A. C. Neves[2], Andre R. Barbosa[3], Jorge M. Branco[4]**

**ABSTRACT:** The nonlinear behaviour of connections between structural elements is critical to the performance of mass-timber structures under seismic loads. However, limited work has been developed in nonlinear modelling and fragility assessment of mass-timber structures. To improve the accuracy of this approach, in particular when considering structures with ring-doweled moment-resisting connections, a nonlinear modelling approach and fragility assessment are proposed and a prototype example of a three-story building is analysed herein as a case study. For the case study, connections and members were designed following the prescriptions in Eurocode 5 and Eurocode 8, considering a high ductility structure. The mechanical properties of the structure are modelled as random variables to evaluate the impact of uncertainty on the prediction of the structural performance, in particular, on the probability of occurrence of ductile and brittle failure modes. The structure is studied under both nonlinear static analysis and multi-record incremental dynamic analysis. From these, fragility curves for different damage levels are computed and a *q*-factor is proposed. Results indicate that the requirements of Eurocode 5 and Eurocode 8 are sufficient to guarantee adequate performance for this type of structure, albeit these may be overconservative. Moreover, it is shown that uncertainties in material properties have a significant impact on the collapse capacity of these structures.

**KEYWORDS:** Fragility Functions, Ring-Doweled Connections, Seismic Assessment, Timber Moment Frames

## 1 INTRODUCTION

Due to the brittle nature of most common failure modes in timber elements, ductility of timber structures is usually a result of the ductility of structural connections. The seismic design of timber structures focuses on guaranteeing that large inelastic deformations occur at the connections, by increasing the slenderness of connectors, and thereby ensuring that yielding of these connectors occurs before any brittle failure mode. In spite of being critical to the seismic performance of timber structures, the inelastic behaviour of connections is not directly taken into account in the design process. Instead, the capacity of a structure to dissipate energy is modelled using seismic response modification factors, such as the *R*-factor or the *q*-factor. The *q*-factor, which is also known as the "behaviour factor", depends on the local ductility of elements and connections and the structural redundancy [1,2]. For timber structures, large displacements can be developed in the connections when slender dowels are used and well-designed detailing guarantees that brittle failure modes (e.g., splitting) are prevented. The level of detailed information regarding timber structures is lower than the one for steel and concrete structures, leading to definitions of *q*-factors in the Eurocode 8 (EC8) [3] that have a wider range of application. In fact, EC8 does not account for the overstrength or the type of connections when quantifying the *q*-factor in timber structures. Moreover, only the most common building structural typologies are referenced in EC8, and no information is provided for structures composed of mass-timber frame structures built with glue laminated or cross-laminated timber (CLT). Limited research exists on the quantification of the ductility and overstrength properties of innovative timber structures (e.g. [4-6]). However, these studies neglect the effect of material uncertainties on ductility and overstrength, and on the response modification/behaviour factors. The development of fragility curves for these structures is not part of the scope of the previous studies as well.

## 2 OBJECTIVE

The main objective of this work is to present results on the performance of mass-timber structures designed with ring-doweled moment resisting connections under seismic loading due to earthquake ground shaking. The performance of this structural typology is quantified by estimating the behaviour *q*-factor, which is computed using multi-record incremental dynamic analysis of nonlinear finite element models that explicitly consider the nonlinear behaviour of the ring-doweled connections, and by presenting a set of immediate occupancy, life-

[1]Leonardo Rodrigues, University of Minho, Portugal, leonardofgrodrigues@gmail.com
[2]Luís A. C. Neves, University of Nottingham, United Kingdom, Luis.Neves@nottingham.ac.uk
[3]Andre R. Barbosa, Oregon State University, United States, Andre.Barbosa@oregonstate.edu
[4]Jorge M. Branco, University of Minho, Portugal, jbranco@civil.uminho.pt

safety, and collapse prevention fragility curves for a case study of a three-story building.

# 3 METHODS

## 3.1 NUMERICAL MODELLING

A range of models has been developed for connections in timber structures considering different scales of analysis. Micro-models focus on the modelling of individual fasteners to a great level of detail (e.g. [7]), while meso-models consider an entire connection composed of several fasteners (e.g. [8]). Macro-models can be used to represent the behaviour of components of a structure or the entire structure. When the objective is to analyse a structure, meso-models represent the best balance between accuracy and detail versus computational cost. In this study, the meso-models considered consist in nonlinear rotational elements that represent the macro response of connections between mass-timber beams and columns. The timber elements are modelled as linear elastic beam-column elements.

These meso-models used here are calibrated with experimental tests' results available in the literature. Existing experimental results on the response of moment-resisting connections indicate that these present a pinched behaviour with stiffness and strength degradation (e.g. [9-11]). These characteristics are similar to those observed in reinforced concrete and steel structures. As a result, it is possible to use models and implementations initially meant for other materials, such as those presented in [12] and [13]. In this study, the Open System for Earthquake Engineering Simulation (OpenSees) finite element package [14] is used, due to its flexibility, extensive library of nonlinear models, and efficiency. OpenSees includes a force-deformation model proposed by [15] known as *Pinching4*. The *Pinching4* model can be used to model a pinched load-deformation response and includes three modes of cyclic degradation: i) strength degradation, ii) unloading stiffness degradation, and iii) reloading stiffness degradation. The experimental results on ring-type doweled mass-timber connections tested by [9] are used to calibrate the *Pinching4* model for use in the nonlinear structural model of the case study building.

## 3.2 FINITE ELEMENT MODELLING AND ANALYSIS

The beams and columns were modelled using linear elastic frame elements connected with zero-length springs. The springs moment-rotation relationship is characterized by the *Pinching4* as shown in Figure 1. Geometric nonlinearities are taken into account by considering P-Delta effects. Rayleigh damping with a damping ratio $\xi = 2\%$ is assigned to the model to account for energy dissipation modes other than the one captured through the nonlinear behaviour of connections. Newton-Raphson method is used to solve the system of equations, with a tolerance of $10^{-8}$ on the inner product of the unbalanced load and displacement increments at each iteration [16]. Newmark integration was used considering $\gamma = 0.5$ and $\beta = 0.25$. The time step adopted was equal to 0.002s.

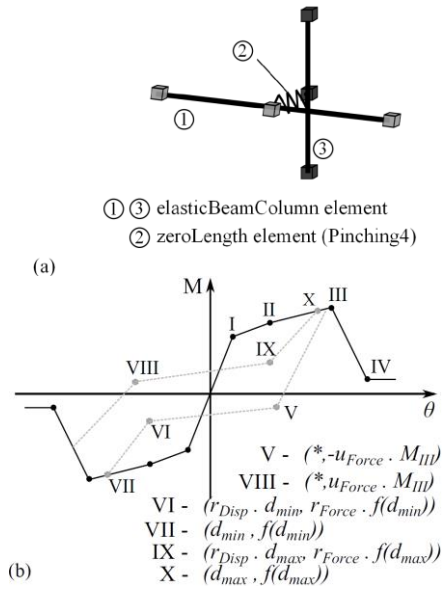


***Figure 1:*** *Numerical model of ring-doweled moment-resisting joint: (a) OpenSees model; (b) Pinching4 parameters.*

## 3.3 CALIBRATION OF HYSTERETIC BEHAVIOUR OF JOINTS

In order to calibrate the constitutive model of the joints, a single-degree-of-freedom model was used to reproduce the results of a fully reversal cyclic test described in [9] shown in Figure 2.

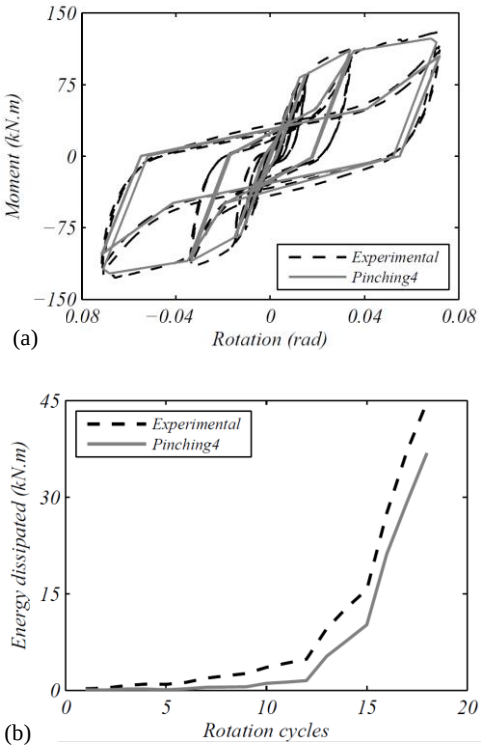


***Figure 2:*** *Comparison between experimental and numerical model results of ring-doweled moment-resisting joint: (a) Experimental test versus numerical results; (b) Energy dissipated: test vs numerical results.*

The *Pinching4* model was selected as it includes pinching, stiffness degradation and strength degradation phenomena observed in the experimental results. This model is defined by a response envelope, unload-reload

rules and three damage rules that control the evolution of the three deterioration mechanisms. The model is defined by 4 moment-rotation *(M-θ)* pairs, defining the 4 states, the rules that control changes between states, and the rules that govern evolution of states. The experimental results indicate that the behaviour of the connection is, as expected considering its geometry, symmetric under hogging and sagging moments. The response envelope was defined by defining points I to IV in Figure 1b, resulting in the values shown in Table 1. Points V to IX were calibrated based on the energy dissipated per cycle as shown in Figure 2b. The cyclic damage is reproduced by the reduction in unloading stiffness, strength and reloading stiffness. The same approach is used to model each effect of damage. Each damage index is given by

$$\delta_i = \left( \alpha_1 \cdot \left( \tilde{d}_{\max} \right)^{\alpha_3} + \alpha_2 \cdot \left( \frac{E_i}{E_{monotonic}} \right)^{\alpha_4} \right) \quad (1)$$

where $\tilde{d}_{\max}$ is given by:

$$\tilde{d}_{\max} = \max\left( \frac{d_{\max,i}}{\text{def}_{\max}}; \frac{d_{\min,i}}{\text{def}_{\min}} \right) \quad (2)$$

and where *i* refers to the current displacement increment, $\alpha_i$ are parameters used to fit the damage rules to the experimental data, *E* is the hysteretic energy and $E_{monotonic}$ is the energy required to achieve failure under monotonic loading. The values $\text{def}_{max}$ and $\text{def}_{min}$ are, respectively, the positive and negative deformations that define failure, and $d_{max,i}$ and $d_{min,i}$ are, respectively, the overall maximum and minimum deformation demands achieved until increment *i*. In [17] and [18], each parameter of *Pinching4* model is presented with more details.

***Table 1:*** *Points used to define the force-deformation response backbone curve for the ring-doweled beam-column connections.*

| Point | $M_i$ (kN.m) | $\theta_i$ (rad) |
|---|---|---|
| I | 83.9 | 0.012 |
| II | 114.5 | 0.034 |
| III | 128.6 | 0.068 |
| IV | 16.8 | 0.129 |

### 3.4 UNCERTAINTY IN TIMBER PROPERTIES

Timber, as a natural material, presents significant variability in its engineering properties. This variability can significantly affect the strength of both members and connections and, eventually, alter the structural failure mode from a ductile to a brittle mode. In this study, this is addressed by defining the properties of timber using probability distributions. A total of 7 variables were defined as probabilistic (see Table 2). Their probability distributions were computed based on the properties of three reference properties: bending strength, bending modulus of elasticity, and density or specific gravity. The probabilistic models for these variables were defined using the characteristic values available in [19] and EN14080 [20] for homogeneous GL24h. The distributions for all other random variables were defined based on procedures proposed in [19].

***Table 2:*** *Random variables for timber material properties*

| X | Dist. | E[X] | CoV[X] | Description |
|---|---|---|---|---|
| $R_m$ | LN | 31 | 0.15 | Bending strength parallel to the grain (MPa) |
| $E_m$ | LN | 11500 | 0.13 | Bending modulus of elasticity (MPa) |
| $\rho_{den}$ | N | 420 | 0.1 | Density (kg/m$^3$) |
| $R_{t,0}$ | LN | 18.6 | 0.18 | Tension strength // to the grain (MPa) |
| $R_{c,0}$ | LN | 23.4 | 0.12 | Compression strength // to the grain (MPa) |
| $G_v$ | LN | 718.8 | 0.13 | Shear modulus (MPa) |
| $R_v$ | LN | 3.12 | 0.15 | Shear strength (MPa) |

The correlation between properties of each structural element was defined following the JCSS Probabilistic Model Code [19]. The correlation between the same property in different elements was assumed equal to 0.8.
The strength and stiffness of the connections was computed considering the expression presented in Eurocode 5 (EC5) [21], taking into account the probabilistic distribution of the random variables. However, the expression proposed in the EC5 for the stiffness of connections estimates significantly higher values than the ones determined from the experimental tests. For this reason, the expression in EC5 was used with a bias factor of 0.55. The strength of the connection was computed using a simplified distribution of forces in the fasteners, and the strength of each fastener was computed using Johansen expression [22]. Again, a significant difference was found between the predicted and the observed strength of the connections. As for stiffness, a bias factor equal to 0.83 was considered. Further details on the computation of stiffness and strength of the connection are provided in [2].
There is no information in the literature on the probabilistic distribution of the parameters defining the nonlinear behaviour of the connection, modelled using the *Pinching4* model. In addition, the number of experimental tests available is insufficient for estimating these parameters with any degree of confidence. For this reason, a simplified approach was used, considering a lognormal distribution, assuming the mean value is equal to the experimentally observed values, and using a large coefficient of variation (CoV = 40%) to take into account the lack of knowledge.

### 3.5 FRAGILITY CURVES

Fragility curves represent the conditional distribution of the probability of failure (e.g., probability of exceeding a specific drift, damage or collapse threshold) as a function of one or more hazard intensity measures (e.g., peak ground acceleration). Fragility curves can be computed using: expert judgment, empirical methods, analytical methods, or hybrid methods that combine two or more of the first three methods [23]. It is commonly accepted that fragility curves follow a lognormal distribution function (e.g. [24-26]). The parameters of this function can be determined using the Monte-Carlo

simulation. In Monte-Carlo simulation a large set of samples is generated, following the joint probability distribution of all random variables. Each sample is analysed as in a deterministic problem, and the value of the limit state function is computed for each sample. The probability of failure is then given by the ratio between the number of failures and the total number of structures.

# 4 CASE STUDY

## 4.1 BUILDING DESCRIPTION

The structure under analysis is a three-story building constructed using a timber moment resisting frame. The structure was designed in [27]. Beams and columns are built using GL24h glue laminated timber, and ring-doweled connections are designed to link beams and columns. In this study, it was assumed that the structure would be built in a site in Lisbon, Portugal, and the structural safety was re-evaluated using EC5 and EC8 for that specific site. The structure was designed aiming at a ductility level compatible with High Ductility Class (DCH) as defined in EC8. The geometry of the structure and its structural components are shown in Figures 3 and 4.

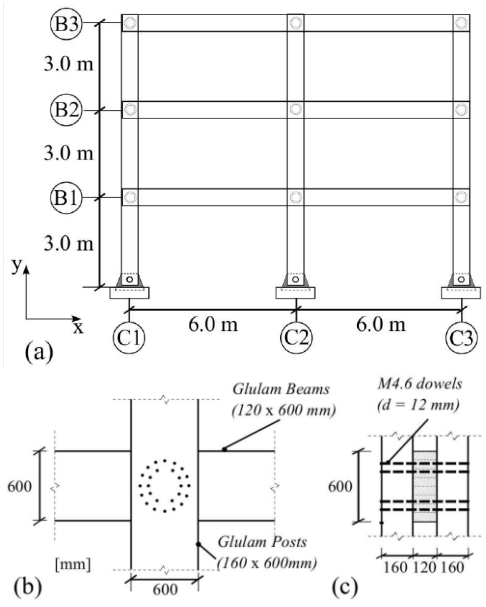


***Figure 3:*** *Two story building with ring-doweled moment-resisting joints: (a) elevation; (b) moment resisting joints detailing.*

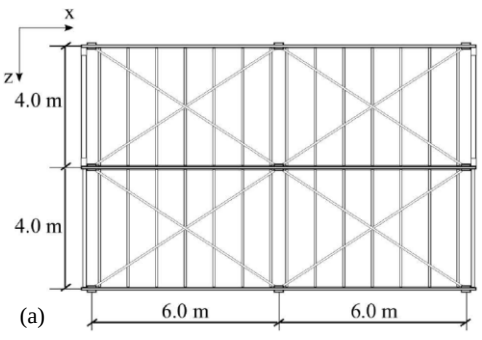


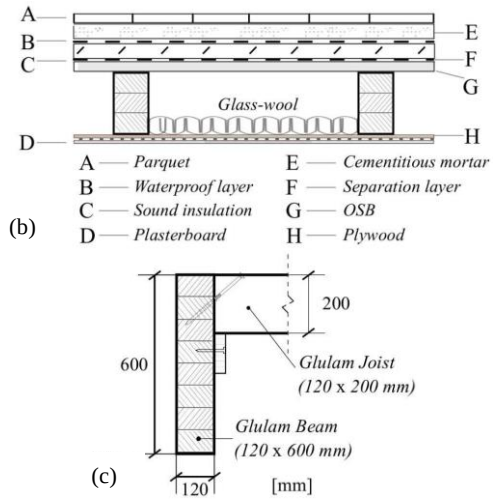


***Figure 4:*** *Traditional floor assemble structure: (a) floor plan; (b) floor components;(c) joists-to-beam connections.*

## 4.2 PUSHOVER ANALYSIS

In a first step, the structure was analysed through a nonlinear static (pushover) analysis. A set of 1000 structural models were generated using Latin Hypercube sampling (LHS), leading to capacity curves shown in Figure 4a. The capacity curve of each structure was approximated by a bilinear curve), as shown in Figure 4b, using the Energy Equivalent Elastic Plastic method [12].

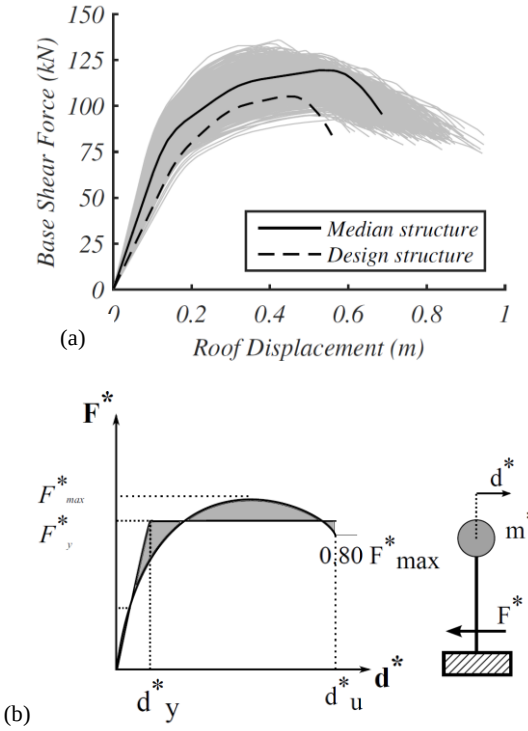


***Figure 5:*** *Nonlinear static analysis: (a) Capacity curves; (b) Equivalent bilinear inelastic model*

By using the results obtained from the pushover curves and applying the *q*-factor definition proposed in [27], it was possible to determine the distribution of *q*-factors for the structural set. As shown in Figure 6, the mean *q*-factor value obtained was 7.2, with a CoV of 8.4%.

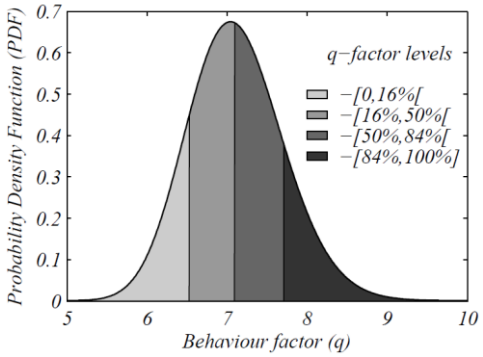


***Figure 5:*** *q*-factor *probability density function (PDF).*

To define fragility curves, thresholds corresponding to Immediate Occupancy (IO), Life Safety (LS) and Collapse Prevention (CP) damage states were first defined. IO was defined as the story drift ratio associated with the first yielding of any connection. LS was defined as any connections reaching the capping rotation $\theta_{III}$ in Figure 1a, while CP corresponds to a 20% decrease from peak capacity estimated from the pushover analysis.

### 4.3 GROUND MOTION SELECTION

A set of 24 ground motion records was extracted from the PEER database (PEER 2012) and scaled to the spectra defined in EC8 for Lisbon, Portugal. According to EC8, two types of seismic spectra must be considered when designing for this site: a large magnitude and far-field earthquake (Type I), and a lower magnitude and near-field earthquake (Type II). The 5% linearly damped response spectra of the scaled ground motions are shown in Figure 6. In addition, the range of periods of interest (i.e., those within 0.3 and 3.0 times the median fundamental period of the structure) are also indicated in Figure 6.

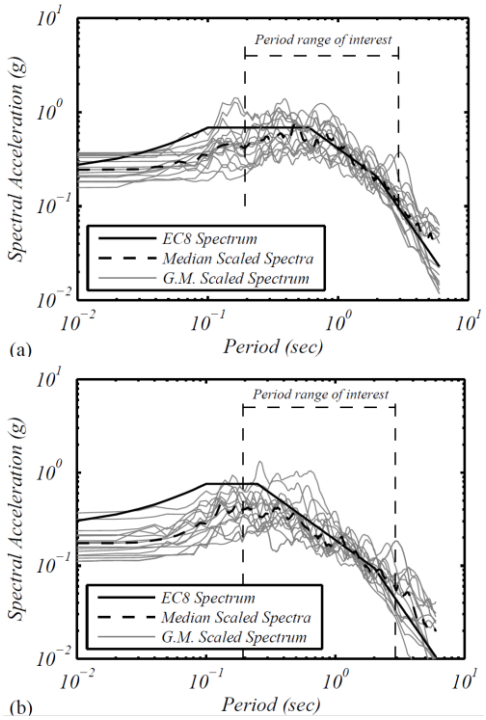


***Figure 6:*** *Response spectra in multi-record IDA: (a) Type I; (b) Type II*

### 4.4 INCREMENTAL DYNAMIC ANALYSIS

Incremental dynamic analysis (IDA) [28] was used to develop the fragility curves. A total of 1000 structure samples were generated based on the assumed random variables and their distributions. Consequently, a total of 24000 curves were generated for the entire structure set. For simplicity, only the results obtained for a median structure are presented in this document. The IDA results obtained for the median structure (i.e. structure considering all random variables set equal to their median value) are presented in Figure 7.

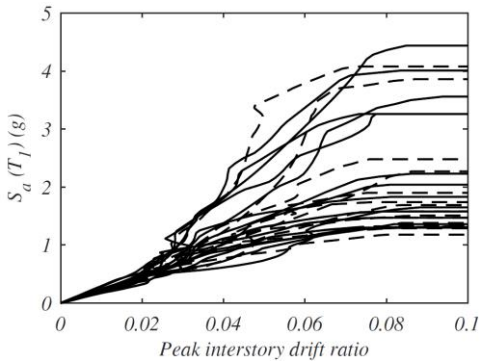


***Figure 7:*** *Set of 24 IDA curves obtained for the analysis of the median structure using the 24 ground motions selected.*

### 4.5 FRAGILITY FUNCTIONS

The spectral accelerations were extracted from the incremental dynamic analysis for each limit state. The fragility curves were computed, for each limit state, by fitting a lognormal distribution to the spectral accelerations leading to the violation of each limit state threshold. Table 3 summarizes the results for the fragility curves for IO, LS and CP damage states, for both the entire sample and the median structure.

***Table 3:*** *Fragility curves parameters for IO, LS and CP Structural set Median structure.*

| Limit state | $\theta_{max}$ | All samples | | Median | |
|---|---|---|---|---|---|
| | | μ (g) | CoV | μ (g) | CoV |
| D > IO | 0.011 | 0.24 | 0.14 | 0.23 | 0.12 |
| | 0.012 | 0.26 | 0.14 | 0.26 | 0.12 |
| | 0.013 | 0.28 | 0.14 | 0.28 | 0.12 |
| D > LS | 0.043 | 1.27 | 0.40 | 1.23 | 0.36 |
| | 0.049 | 1.45 | 0.43 | 1.41 | 0.37 |
| | 0.057 | 1.67 | 0.46 | 1.63 | 0.41 |
| D > CP | 0.071 | 1.93 | 0.50 | 2.00 | 0.49 |
| | 0.079 | 2.01 | 0.51 | 2.11 | 0.51 |
| | 0.088 | 2.04 | 0.51 | 2.15 | 0.51 |

From the parameters presented in Table 3, one can observe that the CoV obtained using all samples is higher than the CoV obtained using only the median properties. The exception refers to the Collapse Prevention Limit State, where the influence of the material uncertainties is not relevant.

The entire sample was segregated in different *q*-factors levels. Thus, in Figure 8, the fragility curves are presented for different *q*-factor levels considering the LS and CP thresholds. It can be seen that the fragility curves associated to high *q*-factor levels present higher variability. In addition, the expected values observed increase with the associated *q*-factor level.

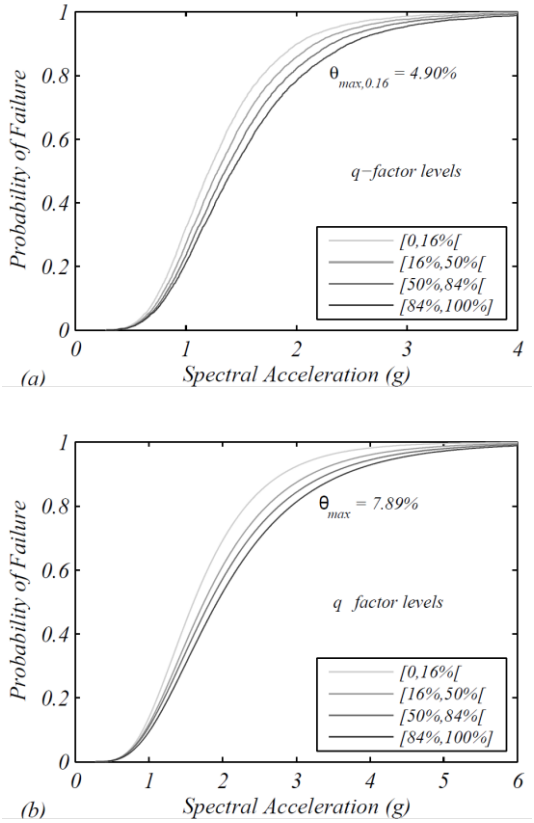


***Figure 8:*** *Fragility curves for different q-*factor *levels: (a) Life Safety; (b) Collapse Prevention*

## 5 CONCLUSIONS

The present paper evaluates the performance of a mass-timber structure with ring-doweled moment resisting connections, under seismic loads. The ring-doweled joints are based on those experimentally studied under cyclic loading in [9]. A three-story building designed according to EC5 and EC8 for a site in Lisbon, Portugal, was analysed. The structure was modelled considering the beams and columns as linear elastic members, while the connections were modelled using the OpenSees *Pinching4* model. The latter model includes pinching and deterioration of stiffness and strength that were calibrated based on the test data available in [9]. The properties of the members and connections were defined taking into account the variability of properties of timber.

Results indicate that considering the uncertainty in the material properties has limited impact on the expected value of the fragility curves. However, it has a significant impact on the coefficient of variation of the fragility curves. Results also indicate that the rules defining the requirements for considering a structure ductile are adequate or potentially too conservative as, even considering uncertainty in material properties and model, all observed failures were ductile.

## ACKNOWLEDGMENTS

This work had financial support of the Portuguese Science Foundation (FCT), through PhD grant PD/BD/113679/2015 included in InfraRisk-PhD program. The results regarding the numerical model for the connections were developed during a Short-term Scientific Mission (STSM) within scope of COST Action FP1101: Assessment, Reinforcement and Monitoring of Timber Structures. Thus, the insightful discussions with Professor Roberto Tomasi and Doctor Andrea Polastri are gratefully acknowledged. The first author would also like to acknowledge the support of Oregon State University during the period in which he was a visiting Ph.D. student, at this institution.

## REFERENCES

[1] Ribeiro F, Barbosa A, Neves L (2014) Application of reliability-based robustness assessment of steel moment resisting frame structures under post-mainshock cascading events. ASCE Journal of Structural Engineering -(140, SPECIAL ISSUE: Computational Simulation in Structural Engineering, A4014008)

[2] Rodrigues L, Branco J, Neves L, Barbosa A (2018) Seismic assessment of a heavy-timber frame structure with ring-doweled moment-resisting connections. Bulletin of Earthquake Engineering 16(3):1341-1371.

[3] CEN (2013) EN 1998-1: Eurocode 8: Design of structures for earthquake resistance Part 1: General rules, seismic actions and rules for buildings. European Committee for Standardisation

[4] Andreolli M, Piazza M, Tomasi R, Zandonini R (2011). Ductile moment-resistant steel-timber connections. Proceedings of the Institution of Civil Engineers-Structures and Buildings 164(2): 65–78.

[5] Ceccotti A, Sandhaas C, Okabe M, Yasumura M, Minowa C, Kawai N (2013). SOFIE project3D shaking table test on a seven-storey full-scale cross laminated timber building. Earthquake Engineering & Structural Dynamics 42(13): 2003–2021.

[6] Gavric I, Frangiacomo M, Ceccoti A (2015) Cyclic behaviour of typical metal connectors for crosslaminated (CLT) structures. Materials and Structures 48(6):1841–1857

[7] Foschi RO (2000) Modeling the hysteretic response of mechanical connections for wood structures.World Conference of Timber Engineering, Whistler, BC, Canada

[8] Rinaldin G, Amadio C, Fragiacomo M (2013) A component approach for the hysteretic behaviour of connections in cross-laminated wooden structures.

[9] Polastri A, Tomasi R, Piazza M, Smith I (2013) Moment resisting dowelled joints in timber structures: mechanical behaviour under cyclic tests. INGEGNERIA SISMICA 30(4):72–81

[10] Folz B, Filiatrault A (2004) Seismic analysis of woodframe structures. ii: Model implementation and verification. Journal of Structural Engineering 130(9):1361–1370

[11] Chui YH, Li Y (2005) Modeling timber moment connection under reversed cyclic loading. ASCE Journal of Structural Engineering 131(11):1757–1763
[12] Foliente GC (1996) Issues in seismic performance testing and evaluation of timber structural systems. Proceedings of the International Wood Engineering Conference, New Orleans, La, pp 28–31
[13] Ibarra LF, Medina RA, Krawinkler H (2005) Hysteretic models that incorporate strength and stiffness deterioration. Earthquake Engineering and Structural Dynamics 34(12):1489–1511
[14] McKenna F, Scott MH, Fenves GL (2009) Nonlinear finite-element analysis software architecture using object composition. Journal of Computing in Civil Engineering 24(1):95–107
[15] Lowes LN, Mitra N, Altoontash A (2003) A beam-column joint model for simulating the earthquake response of reinforced concrete frames. Pacific Earthquake Engineering Research Center, College of Engineering, University of California
[16] Chopra AK, et al (1995) Dynamics of structures, vol 3. Prentice Hall New Jersey
[17] Mazzoni S, McKenna F, Fenves GL (2005) OpenSees command language manual. Pacific Earthquake Engineering Research (PEER) Center, 264.
[18] Park YJ, Ang AHS (1985) Mechanistic seismic damage model for reinforced concrete. ASCE Journal of Structural Engineering 111(4):722–739.
[19] Kohler J, Sørensen JD, Faber MH (2007) Probabilistic modeling of timber structures. Structural Safety 29(4):255–267.
[20] CEN (2005a) EN 14080 Timber structures - Glued laminated timber Requirements. European Committee for Standardisation
[21] CEN (2005b) EN 1995-1-1: Eurocode 5: Design of timber structures Part 1: Common rules and rules for buildings. European Committee for Standardisation.
[22] Johansen K (1949) Theory of timber connections. International Association of Bridge and Structural Engineering, vol 9, pp 249–262.
[23] Porter K (2015) Beginners guide to fragility, vulnerability, and risk. Encyclopedia of Earthquake Engineering pp 235–260
[24] Rosowsky DV, Ellingwood BR (2002) Performance-based engineering of wood frame housing: Fragility analysis methodology. ASCE Journal of Structural Engineering 128(1):32–38
[25] Porter K, Kennedy R, Bachman R (2007) Creating fragility functions for performance-based earthquake engineering. Earthquake Spectra 23(2):471–489
[26] Baker JW (2015) Efficient analytical fragility function fitting using dynamic structural analysis. Earthquake Spectra 31(1):579–599.
[27] Callegari E (2009) Caratterizzazione del comportamento di telai sismoresistenti in legno lamellare. M.S. thesis, Universit`a degli Studi di Trento, Trento, Italia, (in Italian)
[28] Fajfar P (1999) Capacity spectrum method based on inelastic demand spectra. Earthquake Engineering & Structural Dynamics 28(9):979–994.
[29] D. Vamvatsikos and C.A. Cornell, "Incremental dynamic analysis. Earthquake Engineering & Structural Dynamics.", vol. 31, no. 3, pp.491-514, 2002.